NONDESTRUCTIVE FLUORESCENCE LIFETIME IMAGING AND TIME-RESOLVED FLUORESCENCE SPECTROSCOPY DETECT CARTILAGE MATRIX DEPLETION AND CORRELATE WITH MECHANICAL PROPERTIES

A.K. Haudenschild[1], B.E. Sherlock[1], X. Zhou[1], J.C. Hu[2], J.K. Leach[1,3], L. Marcu[1] and K.A. Athanasiou[2,*]

[1] Department of Biomedical Engineering, University of California, Davis, CA, USA
[2] Department of Biomedical Engineering, University of California, Irvine, CA, USA
[3] Department of Orthopedic Surgery, University of California, Davis Medical Center, Sacramento, CA, USA

Abstract

Tissue engineers utilize a battery of expensive, time-consuming and destructive techniques to assess the composition and function of engineered tissues. A nondestructive solution to monitor tissue maturation would reduce costs and accelerate product development. As a first step toward this goal, two nondestructive, label-free optical techniques, namely multispectral fluorescent lifetime imaging (FLIm) and time-resolved fluorescence spectroscopy (TRFS), were investigated for their potential in evaluating the biochemical and mechanical properties of articular cartilage.

Enzymatic treatments were utilized to selectively deplete cartilage of either collagen or proteoglycan, to produce a range of matrix compositions. Samples were assessed for their optical properties using a fiber-coupled optical system combining FLIm and TRFS, their biochemical and mechanical properties and by histological staining. Single and multivariable correlations were performed to evaluate relationships among these properties.

FLIm- and TRFS-derived measurements are sensitive to changes in cartilage matrix and correlate with mechanical and biochemical assays. Mean fluorescence lifetime values extracted from FLIm images (375-410 nm spectral band) showed strong, specific correlations with collagen content ($R^2 = 0.79$, $p < 0.001$) and tensile properties ($R^2 = 0.45$, $p = 0.02$). TRFS lifetime measurements centered at 520 nm (with a 5 nm bandwidth) possessed strong, specific correlations with proteoglycan content ($R^2 = 0.59$, $p = 0.001$) and compressive properties ($R^2 = 0.71$, $p < 0.001$).

Nondestructive optical assessment of articular cartilage, using a combination of FLIm- and TRFS-derived parameters, provided a quantitative method for determining tissue biochemical composition and mechanical function. These tools hold great potential for research, industrial and clinical settings.

Keywords: Cartilage, biomechanics, extracellular matrix, collagens, proteoglycans, imaging, cartilage repair and regeneration, tissue engineering, regenerative medicine.

***Address for correspondence**: Kyriacos A. Athanasiou, PhD, Department of Biomedical Engineering, University of California Irvine, 3418 Engineering Hall, Irvine, CA 92697, USA.
Telephone number: +1 9498249196   Fax number: +1 9498241727   E-mail: athens@uci.edu

Introduction

Tissue engineering of functional replacement tissues requires a strict set of design criteria involving both biochemical and mechanical properties. Currently, tissue engineers, in both research and clinical setting, rely predominantly on destructive and time-consuming techniques that require complete or partial sample loss. Destructive measurements provide valuable information concerning the tissue biochemical and mechanical properties but do not allow spatial or temporal monitoring during tissue development. Furthermore, destructive assays of engineered tissues during *in vivo* experiments require sacrificing the experimental animal, while nondestructive alternatives have the potential to reduce animal use. Clinically, once the replacement tissue has been implanted in the patient, clinicians are often unable to monitor the biochemical and mechanical changes occurring. There is a clear

need for nondestructive methods to evaluate tissue-engineered constructs at all levels of product development (Morgan *et al.*, 2014).

To address these issues, quantitative optical techniques based on endogenous tissue autofluorescence are described for nondestructive tissue imaging and characterization (Gorpas *et al.*, 2015; Gorpas *et al.*, 2016; Sun *et al.*, 2012). Several endogenous biomolecules, including the extracellular matrix (ECM) protein collagen (Georgakoudi *et al.*, 2002) and its crosslinks (Wagnieres *et al.*, 1998), generate tissue autofluorescence. Changes in the fluorescence emission profiles reflect changes in the relative concentration and distribution of individual fluorophores within the tissue. Two optical techniques that are based on fluorescence lifetime (LT) contrast are single-point time-resolved fluorescence spectroscopy (TRFS) – which records the temporal dynamics of ECM autofluorescence at high spectral resolution – and fluorescence lifetime imaging (FLIm) – which maps the surface distribution of the endogenous fluorophores to generate images of the tissue biochemistry. TRFS and FLIm detect biochemical changes in various biological tissues, both *in vitro* and *in vivo* (Fite *et al.*, 2011; Manning *et al.*, 2013; Yankelevich *et al.*, 2014). The combination of TRFS and FLIm in a single apparatus allows for the characterization of cartilage ECM identity, quantity and distribution.

In addition to monitoring changes in biochemical composition, it is also necessary to determine changes in mechanical properties to determine the functionality of both native and engineered replacement tissues. Articular cartilage is a load-bearing tissue and sufficient tensile and compressive properties are critical for the success of engineered replacement tissue (Huey *et al.*, 2012; Makris *et al.*, 2015; Responte *et al.*, 2007). The cartilage ECM is comprised primarily of collagen type II, proteoglycans and water (Zhang *et al.*, 2009) and cartilage mechanical properties are attributed to these ECM components (Setton *et al.*, 1993).

To characterize both the initial materials and the tissue development and maturation that follows, it is essential to have quantitative, validated tools, optimized specifically for articular cartilage tissue engineering applications (Morgan *et al.*, 2014). In the current study, by selectively degrading the individual components of native cartilage ECM, a model for examining the structure-function relationships of articular cartilage and the changes associated with matrix formation/degradation was developed to provide a testing environment for novel diagnostic techniques.

The bacterial enzyme chondroitinase ABC (cABC) effectively degrades all three forms of sulfated glycosaminoglycans (GAGs): chondroitin sulfate, dermatan sulfate and chondroitin-6-sulfate (Hamai *et al.*, 1997). Similarly, bacterial type II collagenase (ColG) degrades native collagen but exhibits broader substrate specificity (Chojkier *et al.*, 1980).

The overall goal of this work was to study whether nondestructive optical methods had the potential to replace the conventional destructive measurements of tissue properties to reduce costs and research time and to allow for time-lapse measurements tracking the maturation of individual samples. Ultimately, endoscopic *in vivo* evaluations of tissue-engineered implants using these nondestructive technologies is desired (Requejo-Isidro *et al.*, 2004).

The current study aimed to deplete the predominant articular cartilage matrix components, collagen and GAG, to measure changes in mechanical, biochemical and optical properties and to form specific, quantitative relationships between destructive and nondestructive measurements. By creating an array of cartilage samples with varying biochemical and mechanical properties, the following questions were addressed: which optical wavelengths were best suited for collagen and proteoglycan quantification, which optical parameters correlated with mechanical properties and wheather the strength of these correlations was sufficient to replace destructive testing methods.

The working hypothesis was that the label-free, nondestructive FLIm and TRFS optical techniques could be used to infer the changes in both biochemical composition and biomechanical properties of articular cartilage over a wide range of matrix compositions.

Materials and Methods

Cartilage harvest

Full thickness cartilage explants (8 mm in diameter) were harvested from the femoral condyles of four juvenile bovine stifle joints (*n* = 19/joint) (Research 87, Boston, MA, USA) (Fig. 1). Samples were trimmed to 2 mm thickness with a custom cutting jig, while preserving the articular surface, and wrapped in gauze soaked in phosphate buffered saline (PBS) (Sigma-Aldrich) with protease inhibitors, as previously described (Agemura *et al.*, 1990). Samples were cycled through three freeze-thaw cycles to lyse cells and stored at −20 °C until treatment and testing.

For comparison of viable and frozen tissue, freshly harvested cylindrical samples (*n* = 6) were cut in cross-section and one half was imaged immediately (viable) while the second half underwent three freeze-thaw cycles (frozen) prior to optical assessment.

Proteolytic enzyme treatments

Cartilage explants were randomly assigned to a treatment group (Griffin *et al.*, 2014; Karchner *et al.*, 2018; Nissi Mj *et al.*, 2016) and placed one sample per well in a 6-well plate (Costar, Corning) in 6 mL of PBS. To remove collagen, type II collagenase (ColG) (Worthington, Lakewood, NJ, USA) was added to a final concentration of 0 (control), 20 (low ColG) or 80 μg/mL (high ColG) per well. Similarly, to remove proteoglycans, chondroitinase ABC (cABC) (Sigma-Aldrich) was added to a final concentration
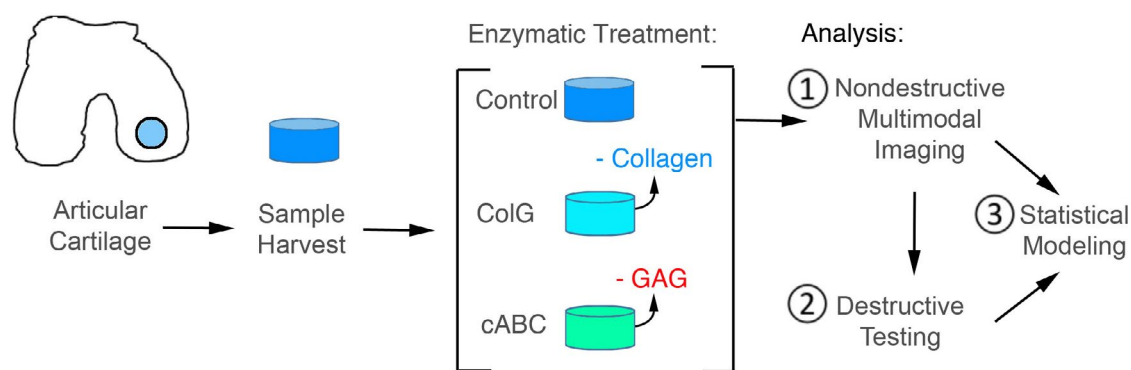
Fig. 1. Schematic diagram of the study. Harvest and treatment of bovine articular cartilage samples in untreated (control), ColG- or cABC-treated groups. Analysis performed on each sample included: 1) nondestructive imaging and spectroscopy (FLIm and TRFS), 2) destructive mechanical (compressive and tensile), biochemical (total collagen and proteoglycan) testing and 3) statistical modeling of measurement correlations to determine significant factors.

of 0 (control), 0.5 (low cABC) or 1 U/mL (high cABC) per well. All treatments included 50 U/mL salt-activated nuclease (ArcticZymes, Tromsø, Norway), 0.02 % ethylenediaminetetraacetic acid (EDTA) (Life Technologies) and 1 % penicillin/streptomycin/ fungizone (Lonza). Sample were treated for 10 h at 37 °C on a rotatory plate at 35 revolutions/min. After treatment, samples were washed in fresh PBS for 12 h to remove residual enzymes.

To determine the applicability of optical assessment on viable tissue, freshly harvested constructs were processed in PBS (control), 80 μg/mL of collagenase (high ColG) or 1 U/mL of cABC (high cABC) as described above.

Non-destructive optical assessment of cartilage
A fiber-based, fluorescence lifetime imaging and spectroscopy system was used for nondestructive assessment of the articular cartilage samples ($n = 6$/condition), followed by biochemical assays, mechanical evaluation and histological processing. The functional principle of operation of the FLIm and TRFS systems is reported by Sun *et al.* (2009) and Yankelevich *et al.* (2014). Time-resolved fluorescence was acquired by both systems using the pulse sampling technique (Marcu *et al.*, 2014) and the decays were parameterized in post-processing using a constrained least-squares deconvolution with Laguerre expansion (Liu *et al.*, 2012). Average lifetimes were calculated using the definition of intensity-weighted average lifetime (Yankelevich *et al.*, 2014). FLIm and TRFS used the same microchip laser (STV-02E-1x0, TEEM photonics, Grenoble, France) that emitted optical pulses at a wavelength of 355 nm to generate sample autofluorescence. Light was delivered to and collected from the sample using a 2 m long, flexible fiber-optic cable (Molex, Lisle, IL, USA) with an outer diameter of 480 μm. During imaging, the distal tip of the fiber was positioned approximately 1 mm above and perpendicular to the articular surface. A two-axis digital translation

stage (MX80L, Parker, Cleveland, OH, USA) was used to scan the fiber across the surface. For optical assessment, the central 5 mm diameter core from each sample was placed in a custom-made, glass sample holder in a PBS bath at room temperature.

FLIm system
For FLIm, the fluorescence emission was separated into four spectral bands (CH1 = 375-410 nm, CH2 = 450-485 nm, CH3 = 515-565 nm, CH4 = 595-660 nm) using a custom-built wavelength selection module. Each spectral band had an associated fiber optic delay line of different lengths (longer wavelength bands have longer delay lines). This arrangement allowed the four spectral bands to be temporally multiplexed onto a single photomultiplier tube (PMT) (R5916U-50, Hamamatsu, Bridgewater, NJ, USA), the voltage from which was digitized using a high-speed data acquisition board (PXIe-5185, National Instruments, Austin, TX, USA) operating with a temporal resolution of 80 ps. This enabled complete mapping of the sample surface in approximately 10 min at a resolution of 20 μm/pixel. The mean and standard deviation of fluorescence lifetime in each spectral band were extracted from the FLIm images by defining circular regions of interest centered on the sample that encompassed > 75 % of the surface area. The significant attenuation of 355 nm light in tissue limits the penetration depth of FLIm to 250-300 μm below the sample surface. To determine the translatability of the technique, viable samples were cut and scanned in cross-section to image depth-dependent changes in fluorescence LT with enzymatic degradation.

TRFS system
For TRFS measurements, a switchable mirror was used to direct the sample fluorescence to a monochromator, which was used to sequentially scan through the full fluorescence spectrum (360-600 nm at 5 nm increments). A PMT at the exit of

the monochromator (MicroHR, Horiba Jobin Yvon, Edison, NJ, USA) was used to record the temporal dynamics of fluorescence at each wavelength. The PMT output was digitized using the same high-speed data acquisition board as the FLIm system. Five distinct points on the sample surface were measured and averaged at each wavelength. The mechanical scanning of the monochromator grating resulted in an acquisition time for TRFS of 30 s per sample.

Biochemical analysis and histology
For biochemical analysis, tissue samples were first measured to obtain wet weights (ww), lyophilized and reweighed to obtain dry weights (dw). Lyophilized samples were digested in papain solution for 18 h at 60 °C, as previously described (Kochiadakis *et al.*, 2001). Sulfated GAG content was assayed using the Blyscan™ Sulfated Glycosaminoglycan Assay kit (Biocolor, Westbury, NY, USA). Total collagen content was quantified using a chloramine-T hydroxyproline assay (Biocolor) (Woessner, 1961). For histological evaluation, samples were fixed in 10 % neutral buffered formalin, paraffin-embedded and sectioned at 10 μm thickness. Sections were stained with hematoxylin and eosin for general morphology, safranin O for glycosaminoglycans or picrosirius red for total collagen following routine procedures. Picrosirius-red-stained collagen was visualized under polarized light microscopy to enhance natural birefringence (Junqueira *et al.*, 1979; Puchtler *et al.*, 1973).

Mechanical testing
Compressive testing was performed on a 2 mm cylindrical punch from each sample, as previously described (Allen and Athanasiou, 2006). Briefly, after height detection was accomplished, a stress relaxation test was performed under conditions of unconfined compression. Samples were equilibrated in a PBS bath, pre-loaded to 0.02 N to ensure contact and preconditioned for 15 cycles of 5 % strain. Next, they were placed under 10 % strain for 600 s and 20 % strain for 900 s. Stress-strain data were analyzed using linear viscoelasticity theory (Mak *et al.*, 1987) in Matlab v2018a (MathWorks, Inc., Natick, MA, USA) to calculate instantaneous modulus, relaxation modulus and coefficient of viscosity for each sample.

Tensile testing was conducted using a uniaxial materials testing machine (Test Resources, Shakopee, MN, USA), as previously described (Makris *et al.*, 2013). Briefly, each articular cartilage sample was cut into a dog-bone shaped tensile specimen, photographed (Canon EOS 7D camera) and thickness and width were measured using ImageJ software (NIH) (Schindelin *et al.*, 2015). A uniaxial strain to failure test was conducted at a strain rate of 1 % of the gauge length/s. Young's modulus was calculated by least squares fitting the linear portion of the resulting stress-strain curve in Matlab.

Statistical analysis and modeling
All evaluations were performed using $n = 6$ samples per treatment group. Data are presented as mean ± standard deviation. Statistical analysis was performed using one-way ANOVA with Tukey's *post hoc* analysis. Significant differences ($p < 0.05$) are indicated by bars not sharing the same letter. For comparison between samples pre- and post-freeze, a matched paired *t*-test was used and significant differences ($p < 0.05$) are indicated by an asterisk.

Correlations between bivariate parameters of each enzymatic treatment were modeled separately to determine which outcome parameter correlated with which biochemical component using simple linear least squares regression analysis. Multivariable linear regression modeling was performed on the entire data set to determine the strength of the effect that multiple independent variables had on a single dependent outcome measurement. To determine which ECM components had significant effects on mechanical and imaging properties, collagen and GAG were modeled as the explanatory variables against 20 % relaxation modulus and Young's modulus (Fig. 5) or average lifetimes from FLIm and TRFS (Fig. 6), respectively. To determine which mechanical properties had significant effects on the imaging properties, 20 % relaxation modulus and Young's modulus were modeled as the explanatory variables against average lifetimes from FLIm and TRFS (Fig. 7). The predicted response (solid black line) and the 95 % confidence interval (red dotted curves) for the predicted values are shown for each regression model (Fig. 5-7). To determine the predictive capabilities of the optical system in determining biochemical and mechanical properties, leave-one-out cross validation was performed on all linear models and root mean square error (RMSE) was calculated to determine the error associated with each model (Martens and Dardenne, 1998). All statistical analyses were performed on JMP v12 (SAS Institute, Cary, NC, USA) and cross validation was performed using Matlab.

<div align="center">

Results

</div>

FLIm-derived parameters correlated with collagen depletion in articular cartilage
Nondestructive imaging of the articular surface of ColG-treated samples resulted in an apparent reduction in FLIm CH1 LT with increasing concentrations of ColG (Fig. 2**a**; representative scan). Mean fluorescence LTs in CH2 and CH3 were not significantly altered by ColG treatments ($p = 0.78$ and 0.67, respectively). Thus, only data from FLIm CH1 LT (termed FLIm LT) are presented. The FLIm LT signal within each sample was homogeneous and no voids or defects were detected in any of the samples tested. Quantification of the central region of

interest of ColG-treated samples showed significant reductions in FLIm LT values with increased ColG treatment (Fig. 2**b**; *p* = 0.002).

Collagenase treatment reduced both biochemical content and mechanical properties of articular cartilage
Biochemically, quantification of ColG-treated samples revealed a significantly decreased collagen and GAG content (Fig. 2**c**, *p* = 0.004 and *p* < 0.001, respectively). Collagenase treatment resulted in surface erosion, decreasing both collagen and GAG content, as seen qualitatively through picrosirius red and safranin O staining, respectively (Fig. 2**d**). Mechanically, both

compressive and tensile properties significantly decreased with increased ColG treatment (Fig. 2**e**, 20 % relaxation modulus, *p* < 0.0001; Fig. 2**f**, Young's modulus, *p* = 0.002). Similarly, both instantaneous modulus and coefficient of viscosity significantly decreased with increased ColG treatment (Table 1, both *p* < 0.0001). Collagenase treatment had a significant, dose-dependent decrease in sample hydration (Table 1, *p* = 0.001).

TRFS-derived parameters correlated with proteoglycan depletion in articular cartilage
TRFS measurements of the articular surface of cABC-treated samples detected a significant decrease in
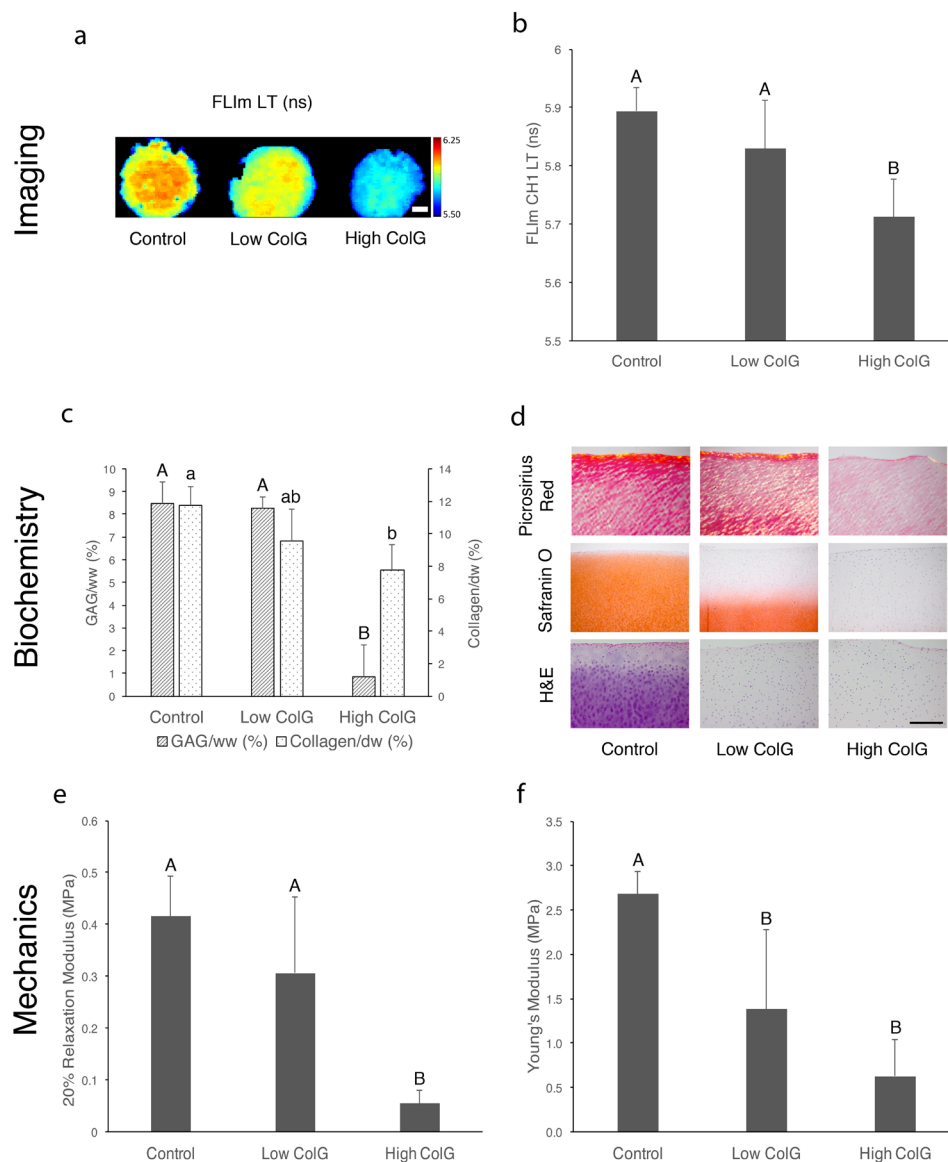

Fig. 2. FLIm-derived parameters correlated with collagen depletion in articular cartilage. (a) Representative FLIm scan of control, low ColG and high ColG corresponding to 0, 20 and 80 µg/mL collagenase treatments (scale bar = 1 mm). (**b**) Average FLIm LT decreased with collagenase treatment. (**c**) Collagen and GAG content decreased with collagenase treatment. (**d**) Picrosirius red and safranin O staining decreased with collagenase treatment. Hematoxylin and eosin staining showed morphological changes (scale bar = 200 µm). (**e**) Compressive modulus and (**f**) tensile modulus decreased with collagenase treatment.

Table 1. Effects of enzymatic treatments on articular cartilage dry weight (DW), wet weight (WW), hydration, instantaneous modulus and coefficient of viscosity (mean ± standard deviation).

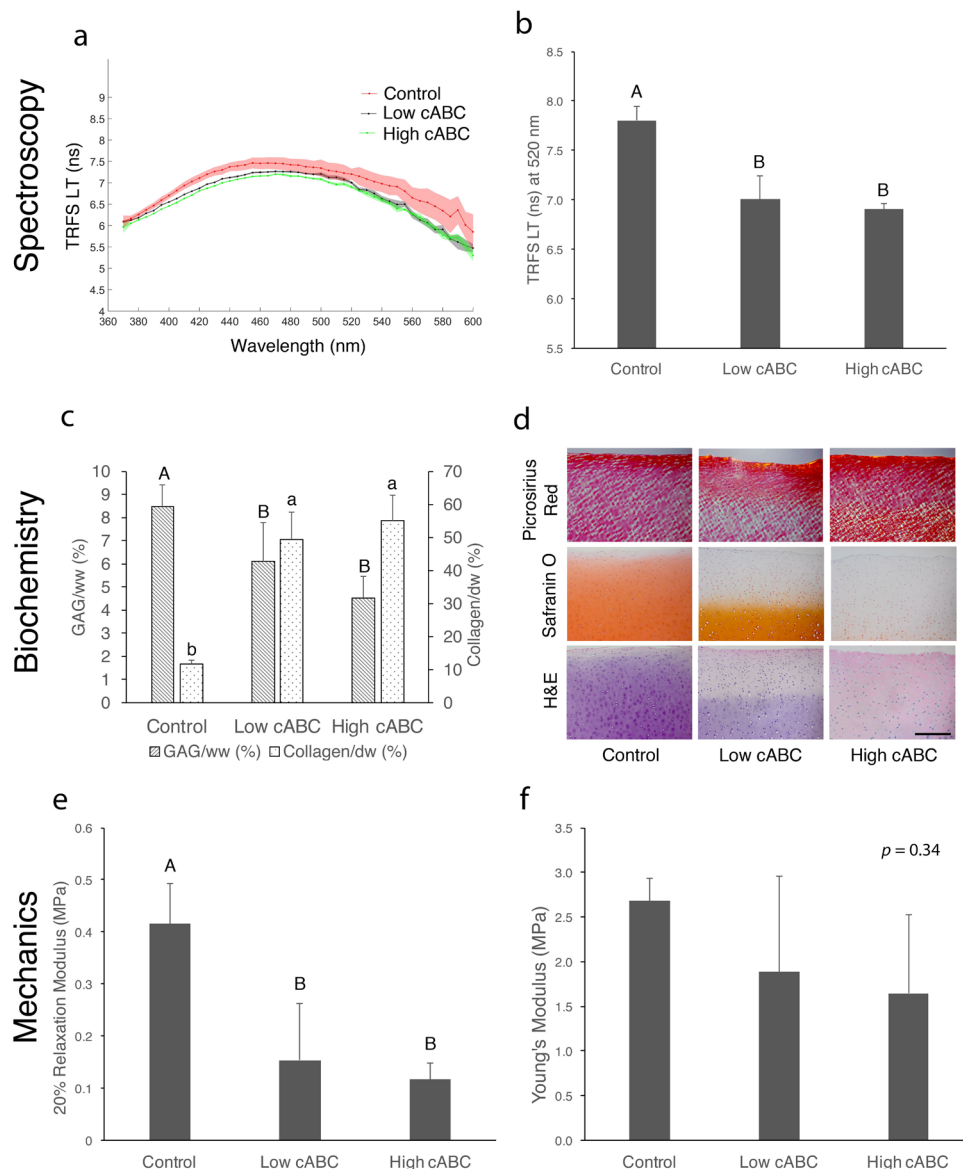| Treatment	DW (mg)	WW (mg)	Hydration (%)	20 % instantaneous modulus (MPa)	Coefficient of viscosity (MPa × s)
Control	1.3 ± 0.2	6.0 ± 0.7	63.6 ± 5.6	6.1 ± 0.9	53.0 ± 3.9
Low ColG	1.7 ± 0.2	6.3 ± 0.6	58.1 ± 9.0	5.9 ± 1.3	36.2 ± 7.9
High ColG	1.6 ± 0.4	6.2 ± 1.3	49.3 ± 8.0	1.5 ± 1.1	4.4 ± 4.5
Low cABC	1.5 ± 0.5	5.9 ± 0.9	72.0 ± 3.5	1.2 ± 0.9	5.1 ± 4.7
High cABC	0.9 ± 2.8	2.8 ± 1.1	74.1 ± 6.5	0.8 ± 0.4	3.2 ± 2.1

Fig. 3. TRFS-derived parameters correlated with proteoglycan depletion in articular cartilage. (**a**) Representative TRFS scan of control, low cABC and high cABC corresponding to 0, 0.5 and 1 U/mL cABC treatments. (**b**) TRFS LT at 520 nm decreased with collagenase treatment. (**c**) Collagen content increased and GAG content decreased with cABC treatment. (**d**) With cABC treatment, picrosirius red increased, safranin O staining decreased and hematoxylin and eosin staining showed morphological changes (scale bar = 200 μm). (**e**) Compressive modulus decreased whereas (**f**) tensile modulus did not significantly change with cABC treatment.

lifetime in the 520 ± 5 nm region of the spectrum. Thus, only data from TRFS LT signal at 520 ± 5 nm (termed TRFS LT) are presented. The reduction in TRFS LT correlated with increased concentrations of cABC (Fig. 3**a**; representative image). Quantification of TRFS LT in cABC-treated samples showed significant reductions in TRFS LT values with increased cABC treatment (Fig. 3**b**; $p < 0.001$).

cABC treatment altered both biochemical content and compressive properties of articular cartilage
Biochemically, quantification of cABC-treated samples showed a significant increase in collagen content and a decrease in GAG content with increased cABC concentrations (Fig. 3**c**, $p = 0.004$ and $p < 0.001$, respectively). cABC treatment resulted in surface erosion of GAG, as seen qualitatively through a decreased safranin O staining, and an increase in collagen staining, as observed in picrosirius red staining (Fig. 3**d**). Mechanically, compressive properties significantly decreased with increased cABC treatment (Fig. 3**e**, 20 % relaxation modulus, $p < 0.0001$) while tensile properties were not significantly affected by either low or high cABC treatment (Fig. 3**f**, Young's modulus, $p = 0.34$). Similarly, both the instantaneous modulus and the coefficient of viscosity significantly decreased with increased cABC treatment (Table 1, both $p < 0.0001$).

cABC treatment resulted in a significant, dose-dependent increase in sample hydration (Table 1, $p = 0.03$).

Combined FLIm- and TRFS-derived parameters were sensitive to changes in cartilage matrix and correlated with destructive mechanical and biochemical assays
Bivariate analysis of ColG-treated samples revealed significant, linear correlations between FLIM LT and collagen content (Fig. 4**a**, $R^2 = 0.79$, $p < 0.001$) and between FLIM LT and Young's modulus (Fig. 4**b**, $R^2 = 0.45$, $p = 0.02$). Cross-validation of FLIm-based predictions of collagen content and Young's modulus determined the RMSE to be 1.15 and 0.9, respectively.

Bivariate analysis of cABC-treated samples revealed significant, linear correlations between TRFS LT and GAG content (Fig. 4**c**, $R^2 = 0.69$, $p = 0.001$) and between TRFS LT and compressive modulus (Fig. 4**d**, $R^2 = 0.76$, $p < 0.001$). Cross-validation of TRFS-based predictions of GAG content and compressive modulus determined the RMSE to be 1.24 and 0.09, respectively.

Mechanical properties correlated with biochemical content in cartilage
A multivariable linear regression model of all biochemical data against tensile data showed
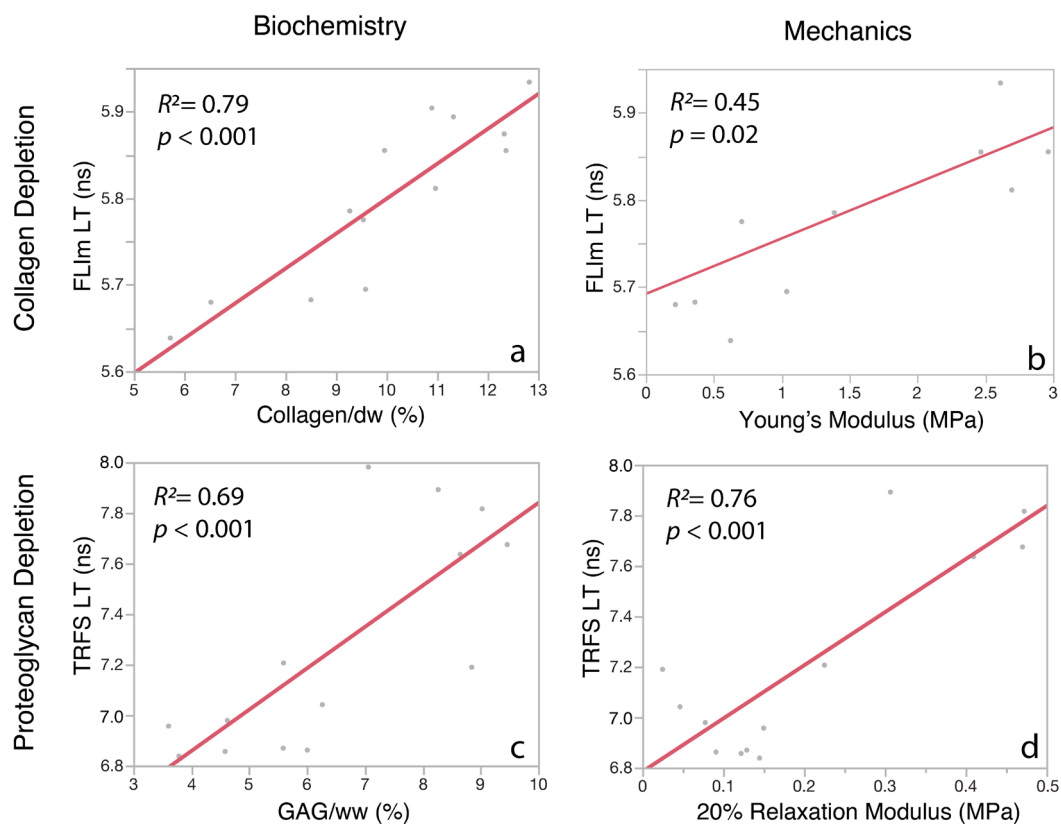

Fig. 4. FLIm- and TRFS-derived parameters correlated with biochemical and mechanical properties in articular cartilage. In collagen-depleted samples, FLIm LT significantly correlated with (**a**) collagen content and (**b**) tensile Young's modulus. In proteoglycan-depleted samples, TRFS LT significantly correlated with (**c**) proteoglycan content and (**d**) compressive relaxation modulus.

that GAG content was not a significant effect in determining Young's modulus (Fig. 5**a**; $p = 0.84$). However, increased collagen content significantly increased the Young's modulus (Fig. 5**b**; $p = 0.01$). A multivariable linear regression model of all biochemical data against compression data showed that increased GAG content significantly increased compressive modulus (Fig. 5**c**; $p = 0.002$), but increased collagen content was not a significant effect in determining compressive modulus (Fig. 5**d**; $p = 0.38$).

FLIm-derived parameters correlated with destructive biochemical testing in cartilage
A multivariable linear regression model of all biochemical testing data against FLIm data showed that GAG content was not a significant effect in determining FLIm LT values (Fig. 6**a**; $p = 0.90$), but increased collagen content significantly increased FLIm LT values (Fig. 6**b**; $p < 0.01$). A multivariable linear regression model of all destructive biochemical testing data against TRFS data showed that increased GAG content significantly increased TRFS LT values (Fig. 6**c**; $p = 0.004$), but was not a significant effect in determining TRFS LT (Fig. 6**d**; $p = 0.60$).

FLIm- and TRFS-derived parameters correlated with mechanical properties in cartilage
A multivariable linear regression model of mechanical testing data against FLIm measurements showed that compressive modulus was not a significant effect in determining FLIm LT values (Fig. 7**a**; $p = 0.48$) but increased tensile modulus significantly altered FLIm LT (Fig. 7**b**; $p = 0.02$). A multivariable linear regression model of mechanical testing data against TRFS parameters showed that increased compressive modulus but not increased tensile modulus were significant effects in determining TRFS LT values (Fig. 7**c**, $p = 0.003$ and Fig. 7**d**, $p = 0.75$, respectively).

Freeze-thaw processing produced wavelength specific changes in fluorescence LT in articular cartilage
Freeze-thaw processing resulted in wavelength specific changes in fluorescence LT [Fig. 8**a**; representative images of viable (V) and frozen (F) samples]. Quantification of FLIm LT showed that the freeze-thaw processing resulted in a significant decrease in FLIm CH1 LT (Fig. 8**b**; $p = 0.003$; $\Delta = 0.14$) and a significant increase in FLIm CH2 LT (Fig. 8**b**; $p = 0.003$; $\Delta = 0.11$) and FLIm CH3 LT (Fig. 8**b**; $p = 0.003$; $\Delta = 0.22$) as compared to viable tissue.
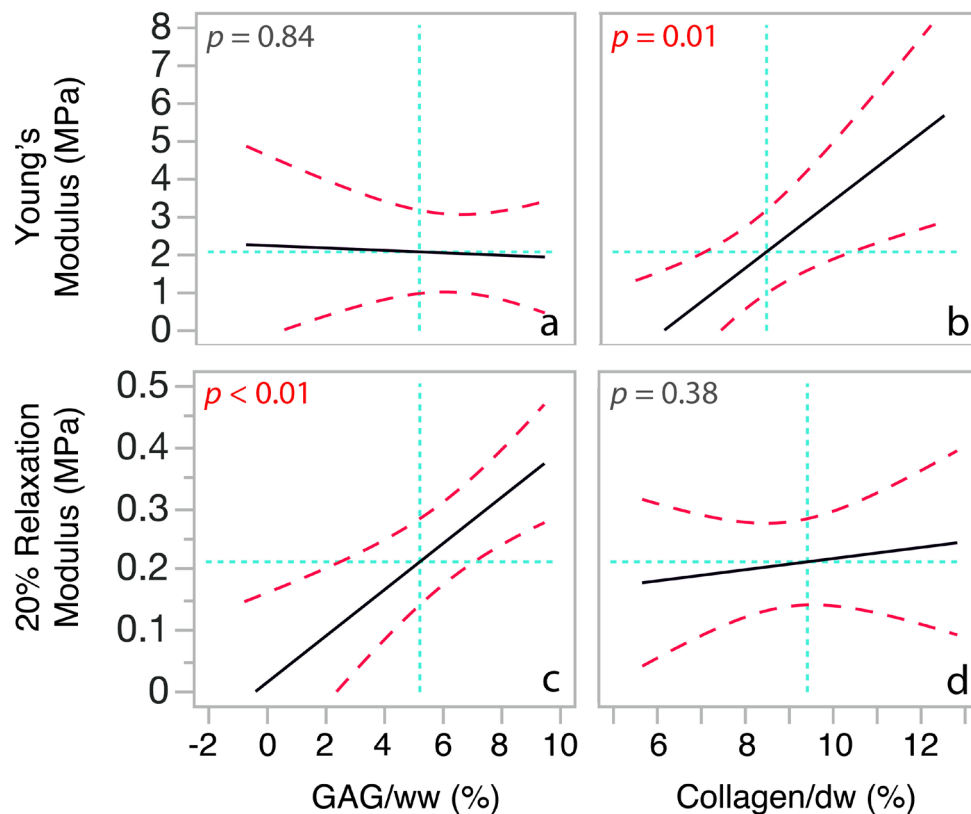

Fig. 5. Mechanical properties correlated with biochemical content. (**a**) GAG content was not a significant effect Young's modulus ($p = 0.84$), while (**b**) increased collagen content significantly increased Young's Modulus ($p = 0.01$). (**c**) Increased GAG content significantly increased compressive modulus ($p < 0.01$), while (**d**) increased collagen content was not a significant effect in determining compressive modulus ($p = 0.38$).
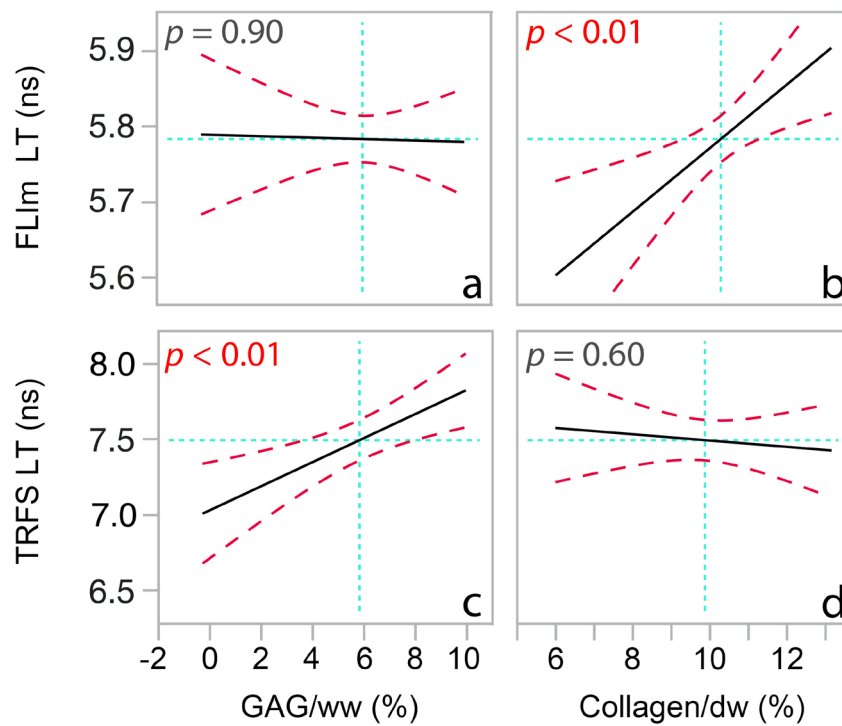
Fig. 6. FLIm- and TRFS-derived parameters correlated with destructive biochemical testing. (**a**) GAG content was not a significant effect in determining FLIm LT values ($p = 0.90$), but (**b**) increased collagen content significantly increased FLIm LT values ($p < 0.01$). (**c**) Increased GAG content significantly increased TRFS LT values ($p < 0.01$), while (**d**) increased collagen content was not a significant effect in determining TRFS LT values ($p = 0.60$).
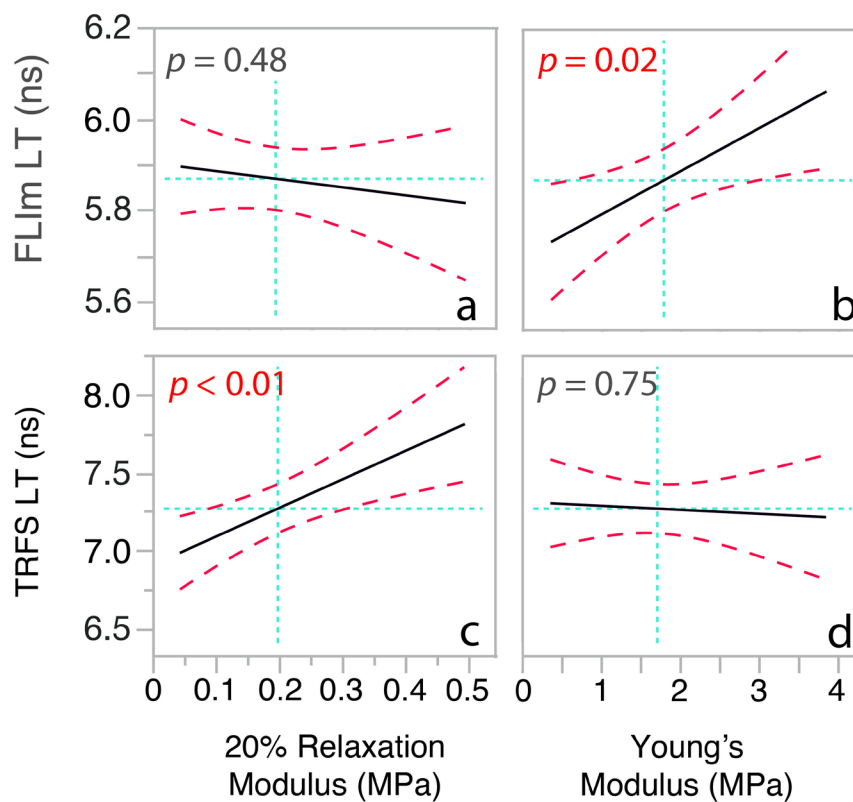

Fig. 7. Optical parameters correlated with mechanical properties in articular cartilage. (**a**) Compressive relaxation modulus was not a significant effect in determining FLIm LT values ($p = 0.48$), but (**b**) increased tensile Young's modulus significantly affected FLIm LT values ($p = 0.02$). (**c**) Increased compressive relaxation modulus significantly affected TRFS LT values ($p < 0.01$), while (**d**) increased tensile Young's modulus was not a significant effect in determining TRFS LT values ($p = 0.75$).

Cross-sectional FLIm imaging of viable cartilage showed depth-dependent changes in enzyme-depleted articular cartilage

Cross-sectional FLIm assessment of viable articular cartilage samples qualitatively showed decreased FLIm CH1 LT at the surface of ColG-treated samples and decreased FLIm CH3 LT at the surface of cABC-treated samples as compared to control (Fig. 8c and 8d, respectively). Decreased FLIm CH1 LT signal correlated with areas of reduced picrosirius red staining in ColG-treated samples with respect to control samples (Fig. 8c; denoted by ‡). Similarly, decreased FLIm CH3 LT signal correlated with areas of reduced safranin O staining in cABC-treated sample with respect to control samples (Fig. 8d; denoted by an asterisk).

<p style="text-align:center">**Discussion**</p>

The results of the present study demonstrated the applicability of using a combination of nondestructive imaging and spectroscopic techniques to determine collagen and proteoglycan content and changes in the tensile and compressive properties of articular cartilage that occur with matrix depletion. The hypothesis that noninvasive assessments could be used to infer the changes in both the biochemical composition and biomechanical properties of cartilage that occur during matrix depletion was supported by the strong linear correlations between destructive and nondestructive tests, making this the first investigation that demonstrated quantitative relationships between fluorescence LT and articular cartilage mechanical properties. The novel findings of this experiment included: 1) quantitative relationships between TRFS LT and both proteoglycan content and compressive moduli and 2) quantitative relationships between FLIm LT and collagen content and tensile modulus. The results of this study are particularly exciting because they can serve as an initial step toward the creation of a nondestructive diagnostic tool for articular cartilage.

The use of enzymatic treatments allowed two objectives to be achieved: 1) the enzymatic treatments mimicked aspects of cartilage degradation under pathology and 2) the treatments yielded samples with varying levels of matrix contents and mechanical properties. Decreases in collagen and GAG content are seen in the early development of osteoarthritis
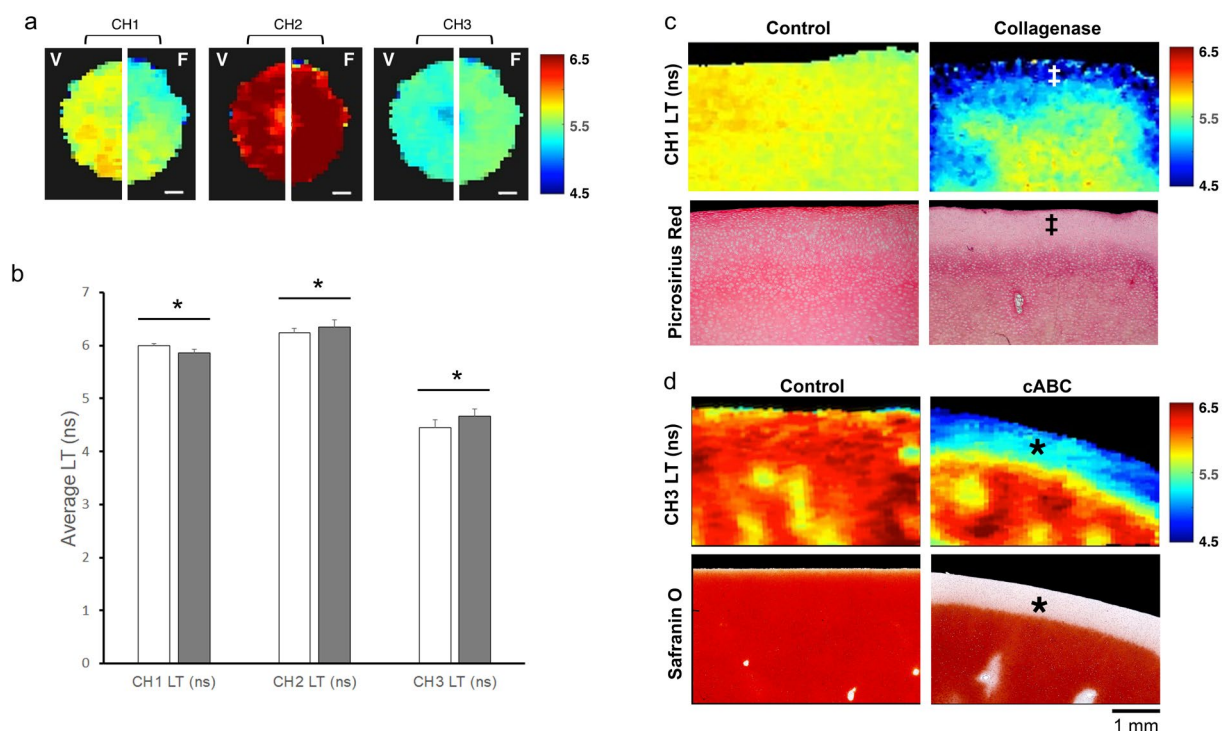

Fig. 8. Comparison between fluorescence LT of viable and freeze-thaw-processed articular cartilage. (**a**) Representative FLIm images of viable (V) articular cartilage and after freeze-thaw processing (F) in each of the three spectral bands (scale = 1 mm). (**b**) Quantification of FLIm LT showed that the freeze-thaw processing (grey bar) resulted in a slight but significant decrease in FLIm CH1 LT ($p = 0.003$; $\Delta = 0.14$) and a significant increase in FLIm CH2 LT ($p = 0.003$; $\Delta = 0.11$) and FLIm CH3 LT ($p = 0.003$; $\Delta = 0.22$) as compared to viable tissue (white bar). (**c**) Cross-sectional fluorescence LT image (CH1: 375-410 nm spectral band) of ColG-degraded articular cartilage showed decreased LT in collagen-depleted regions (‡) that corresponded to less-stained regions in picrosirius red histological sections. (**d**) Cross-sectional fluorescence LT image (CH3: 532-565 nm spectral band) of cABC-degraded articular cartilage showed decreased LT in GAG-depleted regions (*) that corresponded to unstained regions in safranin O histological sections (scale bar = 1 mm).

in articular cartilage (Squires *et al.*, 2003). Similarly, the decrease in cartilage ECM composition created by the enzymatic treatments employed in this study is well established. Collagen and GAG content in articular cartilage treated with the highest dose of ColG were reduced to 66 % and 10 %, respectively, of untreated controls. The reduction in GAG content after ColG treatment was likely due to the inability of matrix with digested collagen to retain the highly charged GAG matrix within the tissue. In cABC-treated cartilage, GAG content was reduced to 53 % of its original value, as similarly reported by Agemura *et al.* (1990). Utilization of both enzymatic treatments caused dose-dependent reductions in matrix components from articular cartilage, creating a range of biochemical and mechanical properties for optical characterization.

The present study reaffirmed the structure-function relationships within articular cartilage, where its material properties are determined by the biochemical composition of the main tissue constituents, GAG and collagen (Setton *et al.*, 1993). Multivariable linear regression models evaluating the effects of collagen content or GAG content showed that the collagen matrix content significantly regulated the tensile response of the cartilage (p = 0.01). A high dose of ColG resulted in a 5-fold decrease in tensile properties. Similarly, multivariable linear regression models found that proteoglycan matrix content significantly affected the compressive response of the cartilage (p < 0.01). A high dose of cABC resulted in a 4-fold decrease in compressive properties. Based on these and prior literature findings (Pritzker *et al.*, 2006), it is expected that changes in cartilage composition and structure, including the depletion of the collagen network and GAGs, result in the impaired functional integrity of the cartilage.

A combination of TRFS and FLIm in a single apparatus was capable of characterizing the identity, quantity and distribution of both collagen and proteoglycans in articular cartilage and of forming quantitative relationships with tissue mechanical properties. The strong correlations between TRFS LT and GAG content (R^2 = 0.59; p = 0.001) and between FLIm LT and collagen content (R^2 = 0.79; p < 0.001) support the use of nondestructive techniques for the quantification of the cartilage biochemical components. While fluorescence lifetime techniques are sensitive to changes in sample biochemistry and do not directly measure tissue mechanical properties, the strong structure-function relationship resulted in strong correlations between each optical assessment technique and specific mechanical properties. TRFS LT had a strong correlation with tissue compressive relaxation modulus (R^2 = 0.71; p < 0.001). Likewise, FLIm LT resulted in a significant correlation with tensile Young's modulus (R^2 = 0.45; p = 0.02). During cABC treatment, GAG removal relatively enriched the collagen content with respect to native tissue values. While the relative collagen content increased

4-fold, the tensile properties were not significantly improved; thus, the optical measurements are not just coincidentally related to the mechanical properties, but also dependent upon ECM structure (Morgan *et al.*, 2014). Because optical properties are attributed not only to the number of molecules present but also to their environment (Marcu *et al.*, 2014), the imaging probe measurements provide more of bulk property of the tissue. By encasing both optical techniques in one probe, it is possible to envision a single, non-destructive tool for measuring both biological content and mechanical properties.

The combination of TRFS and FLIm in a single apparatus exploited the natural complementarity that exists between the two techniques. FLIm is a high-throughput technique that is designed to record the spatial distribution of endogenous fluorophores at high spatial sampling (Marcu *et al.*, 2014). FLIm images typically contain several thousand pixels, allowing the use of statistical methods to detect subtle shifts in fluorescence lifetime. The primary drawback of FLIm is its limited spectral resolution, which reduces its sensitivity to changes in sample fluorescence that are only apparent within narrow regions of the spectrum. TRFS is a point measurement technique that records sample autofluorescence at high spectral resolution (Marcu *et al.*, 2014). Although TRFS does not capture spatial information, a high-resolution measurement of the fluorescence spectrum can identify the spectral regions that provide optimal contrast between groups that other methods cannot detect. This feature could be exploited in the design of future FLIm systems, where the distribution of spectral bands could be determined by TRFS measurements of a particular tissue type. In the case of a dedicated cartilage FLIm system, it is possible to envision designing a custom apparatus with two spectral bands, centered at 390 ± 10 nm and 520 ± 5 nm, for detecting changes in collagen and GAG, respectively.

A range of alternative optical techniques have previously been employed to monitor changes in the structure and biochemistry of articular cartilage. Fourier transform infrared (FT-IR) spectroscopy is successfully used to measure differences in the composition of healthy and osteoarthritic cartilage (Rieppo *et al.*, 2012). While FT-IR can be employed with fiber optics in reflection mode, the method requires a constant level of contact with the tissue sample to produce reliable results and its large probe size limits both *in vivo* access to the joint as well as spatial resolution (Hanifi *et al.*, 2012). These technical challenges need to be resolved before this imaging technique could be readily deployed *in vivo*. Raman spectroscopy can delineate cartilage zonal structure (Bergholt *et al.*, 2016) and detect lipid distribution (Mansfield and Winlove, 2017). While Raman spectroscopy generally utilizes longer excitation wavelengths than 355 nm, resulting in greater penetration depths, it is an inherently slow technique with individual spectra often taking between 0.1-

0.5 s/acquisition (Bergholt *et al.,* 2016). By comparison, FLIm and TRFS acquired complete fluorescent decays imaging data in < 10 ms. The order of magnitude difference in image acquisition speed is critical with respect to the translational potential of FLIm and TRFS over Raman-based approaches. Finally, optical coherence tomography (OCT) is widely used to image articular cartilage microstructure (Nebelung *et al.*, 2015) and is successfully deployed arthroscopically (Liukkonen *et al.*, 2013). This high-speed, high-resolution imaging technique benefits from the enhanced penetration depths afforded by near-infrared light, allowing OCT to resolve cartilage structure between 1-2 mm below the surface. Despite several encouraging developments, OCT lacks biochemical sensitivity and it cannot reliably detect changes in proteoglycan content (Saarakkala *et al.*, 2009). In comparison, the fiber-based FLIm-TRFS imaging platform is designed to rapidly acquire high-resolution images in real time and to ease the translation into human imaging by augmentation of the current clinical practice of arthroscopy. By incorporating the FLIm fiber into a conventional viewing scope, this technique would enable straightforward visual evaluation of the integrity of the cartilage surface, as well as determination of quantitative parameters reflecting the quality of articular cartilage tissue. Furthermore, decreasing the diameter of the optical-probe fiber so that it can be inserted through a standard needle would open the potential for nondestructive evaluation of articular cartilage health as an office procedure. Use of such a minimally-invasive technique for evaluation of cartilage quality could facilitate early intervention and assess the efficacy of rehabilitation programs and therapeutic interventions on cartilage repair.

While the present study focused on the nondestructive evaluation of native cartilage depletion *ex vivo*, these techniques could be employed to execute longitudinal research studies, create more efficient animal studies requiring fewer animal sacrifices, monitor product development in an industrial manufacturing process and quantify clinically cartilage degeneration and repair. The optical system was able to measure changes in articular cartilage composition from scans made perpendicular to the articular surface toward the bone. While this scan direction is the most relevant clinically, there is a limited penetration depth of the system (200-250 µm at wavelengths of 355 nm). That, coupled with the surface erosion of the proteins in the tissue subjected to enzymatic treatments, resulted in lower than expected differences in fluorescence signal. Larger changes in signal are possible by switching to multiphoton excitation of fluorescence (Sherlock *et al.*, 2016). This technique provides intrinsic optical sectioning, confining the extent of the region within which fluorescence is excited to less than 10 µm. Multiphoton excitation of fluorescence has the potential to increase the overall sensitivity of

the device, allowing the system to better discriminate between degraded and healthy cartilage regions.

Freeze-thaw cycles were used to remove the cellular component of the articular cartilage to avoid interference of the cells with imaging modalities. While freeze-thaw processing was able to isolate individual protein contributions to fluorescence LT, it did not fully represent conditions encountered in the final application of this method. Studies on freshly-harvested articular cartilage were conducted to determine whether the optical system could assess a viable tissue. While the freezing process did produce significant changes in fluorescence LT, the changes were small when compared to changes created by matrix degradation (Δ = 1.0 ns for cABC-digestion *vs.* Δ = 0.22 ns for freeze-thaw). These small differences in cellular contribution were most likely due to the low (~ 10 % by volume) composition of cells within articular cartilage. It is possible that the elimination of the low fluorescence LT signal of cells (~2-3 ns) in CH2 and CH3 resulted in an increase in LT in both channels upon cell removal with freeze-thaw processing. The slight decrease in FLIm CH1 was likely due to the breaking of pyridinoline crosslinks by the expansion of intra-fibrillar fluid during ice formation in the freezing process (Ozcelikkale and Han, 2016). Matrix degradation by both ColG and cABC was detectable with FLIm assessment of viable articular cartilage samples and correlated well with histological staining, supporting the use of the optical system in a diagnostic application.

In conclusion, the label-free optical techniques FLIm and TRFS successfully detected collagen and proteoglycan changes in articular cartilage composition in both viable and previously frozen tissues. Using multivariable linear regression models, these complimentary optical techniques were found to be strongly correlated with compressive and tensile properties. Specifically, the FLIm LT optical system could detect changes in collagen content and tensile properties while the TRFS LT optical system could detect changes in GAG content and compressive properties of articular cartilage. The development of nondestructive tools with potential to monitor the functional properties of cartilage is an exciting step forward for both *in vitro* and *in vivo* studies in the future.

and read and approved the final version. The authors have no conflicts of interest to declare.

References

Agemura DH, O'Brien WD, Jr., Olerud JE, Chun LE, Eyre DE (1990) Ultrasonic propagation properties of articular cartilage at 100 MHz. J Acoust Soc Am **87**: 1786-1791.

Allen KD, Athanasiou KA (2006) Viscoelastic characterization of the porcine temporomandibular joint disc under unconfined compression. J Biomech **39**: 312-322.

Bergholt MS, St-Pierre JP, Offeddu GS, Parmar PA, Albro MB, Puetzer JL, Oyen ML, Stevens MM (2016) Raman spectroscopy reveals new insights into the zonal organization of native and tissue-engineered articular cartilage. ACS Cent Sci **2**: 885-895.

Chojkier M, Peterkofsky B, Bateman J (1980) New method for determining the extent of proline hydroxylation by measuring changes in the ratio of [4-3H]:[14C]proline in collagenase digests. Anal Biochem **108**: 385-393.

Fite BZ, Decaris M, Sun Y, Sun Y, Lam A, Ho CK, Leach JK, Marcu L (2011) Noninvasive multimodal evaluation of bioengineered cartilage constructs combining time-resolved fluorescence and ultrasound imaging. Tissue Eng Part C Methods **17**: 495-504.

Georgakoudi I, Jacobson BC, Muller MG, Sheets EE, Badizadegan K, Carr-Locke DL, Crum CP, Boone CW, Dasari RR, Van Dam J, Feld MS (2002) NAD(P) H and collagen as *in vivo* quantitative fluorescent biomarkers of epithelial precancerous changes. Cancer Res **62**: 682-687.

Gorpas D, Fatakdawala H, Bec J, Ma D, Yankelevich DR, Qi J, Marcu L (2015) Fluorescence lifetime imaging and intravascular ultrasound: co-registration study using *ex vivo* human coronaries. IEEE Trans Med Imaging **34**: 156-166.

Gorpas D, Ma D, Bec J, Yankelevich DR, Marcu L (2016) Real-time visualization of tissue surface biochemical features derived from fluorescence lifetime measurements. IEEE Trans Med Imaging **35**: 1802-1811.

Hamai A, Hashimoto N, Mochizuki H, Kato F, Makiguchi Y, Horie K, Suzuki S (1997) Two distinct chondroitin sulfate ABC lyases. An endoeliminase yielding tetrasaccharides and an exoeliminase preferentially acting on oligosaccharides. J Biol Chem **272**: 9123-9130.

Hanifi A, Bi X, Yang X, Kavukcuoglu B, Lin PC, DiCarlo E, Spencer RG, Bostrom MP, Pleshko N (2012) Infrared fiber optic probe evaluation of degenerative cartilage correlates to histological grading. Am J Sports Med **40**: 2853-2861.

Huey DJ, Hu JC, Athanasiou KA (2012) Unlike bone, cartilage regeneration remains elusive. Science **338**: 917-921.

Junqueira LCU, Bignolas G, Brentani RR (1979) Picrosirius staining plus polarization microscopy, a specific method for collagen detection in tissue sections. Histochem J **11**: 447-455.

Kochiadakis GE, Chrysostomakis SI, Kalebubas MD, Filippidis GM, Zacharakis IG, Papazoglou TG, Vardas PE (2001) The role of laser-induced fluorescence in myocardial tissue characterization: an experimental *in vitro* study. Chest **120**: 233-239.

Liu J, Sun Y, Qi J, Marcu L (2012) A novel method for fast and robust estimation of fluorescence decay dynamics using constrained least-squares deconvolution with Laguerre expansion. Phys Med Biol **57**: 843-865.

Liukkonen J, Hirvasniemi J, Joukainen A, Penttila P, Viren T, Saarakkala S, Kroger H, Jurvelin JS, Toyras J (2013) Arthroscopic ultrasound technique for simultaneous quantitative assessment of articular cartilage and subchondral bone: an *in vitro* and *in vivo* feasibility study. Ultrasound Med Biol **39**: 1460-1468.

Mak AF, Lai WM, Mow VC (1987) Biphasic indentation of articular cartilage-I. Theoretical analysis. J Biomech **20**: 703-714.

Makris EA, Gomoll AH, Malizos KN, Hu JC, Athanasiou KA (2015) Repair and tissue engineering techniques for articular cartilage. Nat Rev Rheumatol **11**: 21-34.

Makris EA, MacBarb RF, Responte DJ, Hu JC, Athanasiou KA (2013) A copper sulfate and hydroxylysine treatment regimen for enhancing collagen cross-linking and biomechanical properties in engineered neocartilage. FASEB J **27**: 2421-2430.

Manning HB, Nickdel MB, Yamamoto K, Lagarto JL, Kelly DJ, Talbot CB, Kennedy G, Dudhia J, Lever J, Dunsby C, French P, Itoh Y (2013) Detection of cartilage matrix degradation by autofluorescence lifetime. Matrix Biol **32**: 32-38.

Mansfield JC, Winlove CP (2017) Lipid distribution, composition and uptake in bovine articular cartilage studied using Raman micro-spectrometry and confocal microscopy. J Anat **231**: 156-166.

Marcu L, French PMW, Elson DS (2014) Fluorescence lifetime spectroscopy and imaging: principles and applications in biomedical diagnostics. CRC Press/Taylor & Francis Group, Boca Raton, FL, USA.

Martens HA, Dardenne P (1998) Validation and verification of regression in small data sets. Chemometr Intell Lab Syst **44**: 99-121.

Morgan SP, Rose FR, Matcher SJ (2014) Optical techniques in regenerative medicine. Taylor & Francis, Boca Raton, FL, USA.

Nebelung S, Brill N, Marx U, Quack V, Tingart M, Schmitt R, Rath B, Jahr H (2015) Three-dimensional imaging and analysis of human cartilage degeneration using optical coherence tomography. J Orthop Res **33**: 651-659.

Ozcelikkale A, Han B (2016) Thermal destabilization of collagen matrix hierarchical structure by freeze/thaw. PLoS One **11**: DOI: 10.1371/journal.pone.0146660.

Pritzker KPH, Gay S, Jimenez SA, Ostergaard K, Pelletier JP, Revell PA, Salter D, van den Berg WB (2006) Osteoarthritis cartilage histopathology: grading and staging. Osteoarthritis Cartilage **14**: 13-29.

Puchtler H, Waldrop FS, Valentine LS (1973) Polarization microscopic studies of connective tissue stained with picro-sirius red FBA. Beitr Pathol **150**: 174-187.

Requejo-Isidro J, McGinty J, Munro I, Elson DS, Galletly NP, Lever MJ, Neil MAA, Stamp GWH, French PMW, Kellett PA, Hares JD, Dymoke-Bradshaw AKL (2004) High-speed wide-field time-gated endoscopic fluorescence-lifetime imaging. Optics Letters **29**: 2249-2251.

Responte DJ, Natoli RM, Athanasiou KA (2007) Collagens of articular cartilage: structure, function, and importance in tissue engineering. Crit Rev Biomed Eng **35**: 363-411.

Rieppo L, Rieppo J, Jurvelin JS, Saarakkala S (2012) Fourier transform infrared spectroscopic imaging and multivariate regression for prediction of proteoglycan content of articular cartilage. PLoS One **7**: DOI: 10.1371/journal.pone.0032344.

Saarakkala S, Wang SZ, Huang YP, Zheng YP (2009) Quantification of the optical surface reflection and surface roughness of articular cartilage using optical coherence tomography. Phys Med Biol **54**: 6837-6852.

Schindelin J, Rueden CT, Hiner MC, Eliceiri KW (2015) The ImageJ ecosystem: an open platform for biomedical image analysis. Mol Reprod Dev **82**: 518-529.

Setton LA, Mow VC, Muller FJ, Pita JC, Howell DS (1993) Altered structure-function relationships for articular cartilage in human osteoarthritis and an experimental canine model. Agents Actions Suppl **39**: 27-48.

Sherlock B, Yu F, Stone J, Warren S, Paterson C, Neil MA, French PM, Knight J, Dunsby C (2016) Tunable fibre-coupled multiphoton microscopy with a negative curvature fibre. J Biophotonics **9**: 715-720.

Squires GR, Okouneff S, Ionescu M, Poole AR (2003) The pathobiology of focal lesion development in aging human articular cartilage and molecular matrix changes characteristic of osteoarthritis. Arthritis Rheum **48**: 1261-1270.

Sun Y, Park J, Stephens DN, Jo JA, Sun L, Cannata JM, Saroufeem RM, Shung KK, Marcu L (2009) Development of a dual-modal tissue diagnostic system combining time-resolved fluorescence spectroscopy and ultrasonic backscatter microscopy. Rev Sci Instrum **80**: 065104.

Sun Y, Responte D, Xie H, Liu J, Fatakdawala H, Hu J, Athanasiou KA, Marcu L (2012) Nondestructive evaluation of tissue engineered articular cartilage using time-resolved fluorescence spectroscopy and ultrasound backscatter microscopy. Tissue Eng Part C Methods **18**: 215-226.

Wagnieres GA, Star WM, Wilson BC (1998) *In vivo* fluorescence spectroscopy and imaging for oncological applications. Photochem Photobiol **68**: 603-632.

Woessner JF Jr. (1961) The determination of hydroxyproline in tissue and protein samples containing small proportions of this imino acid. Arch Biochem Biophys **93**: 440-447.

Yankelevich DR, Ma D, Liu J, Sun Y, Sun Y, Bec J, Elson DS, Marcu L (2014) Design and evaluation of a device for fast multispectral time-resolved fluorescence spectroscopy and imaging. Rev Sci Instrum **85**: DOI: 10.1063/1.4869037.

Zhang L, Hu J, Athanasiou KA (2009) The role of tissue engineering in articular cartilage repair and regeneration. Crit Rev Biomed Eng **37**: 1-57.

Discussion with Reviewer

Stephen Waldman: Can the authors comment on the effect of the water content in the tissue samples (as TRFS was highly correlated with GAG content relative to tissue wet weight as opposed to FLIm, which was highly correlated with collagen content relative to tissue dry weight)?

Authors: In this study, all optical measurements were taken on hydrated tissue. The normalization of ECM proteins to wet or dry weight was chosen based on standard reporting conventions and Table 1 allows conversion between the two methods. Because water does not have a detectable fluorescent signal, the water itself does not affect fluorescence the lifetime values used in our analysis.

Stephen Waldman: If the water content of the tissue is not determined, does this pose any limitation to the technique?

Authors: No, we do not see any limitation.

Editor's note: The Scientific Editor responsible for this paper was Stephen Ferguson.